

# More Fairly Distributed Pixel Characteristics of the Principal Image Histogram Components

Watit Benjapolakul<sup>1</sup> and Bongkarn Homnan<sup>2</sup>

<sup>1</sup>Department of Electrical Engineering, Chulalongkorn University

254/1-4 Phayathai Rd., Pathumwan, Bangkok 10330, Thailand

<sup>2</sup>Research Service Center, Dhurakij Pundit University

110/1-4 Prachachuen Rd., Laksi, Bangkok 10210, Thailand

Corresponding author : bongkarn@dpu.ac.th

**Abstract :** Horizontal partitioned on the image histogram, the pixels of light intensity levels are capable to be fairly distributed on any image. This paper emphasizes on the principal light intensity levels including the  $r^{\text{th}}$  order light intensity levels and especially the 1<sup>st</sup> - 3<sup>rd</sup> order principal light intensity levels. The fairness of pixel distribution is categorized based on the quadrant of the coordinate system and the standard deviation of pixels under an environment of the polar coordinate system. The results illustrate higher and high fairnesses of pixel distribution by utilizing the suitable principal light intensity level accompanied with the other  $r^{\text{th}}$  order principal light intensity levels.

**Keywords :** Distribution, fairness, histogram, intensity, principal.

## 1. Introduction

### 1.1 Symbols

<b>L</b>	the light intensity level set		limited by the maximum light intensity level
<b>m<sub>l</sub></b>	the light intensity level member set	$\bar{x}$	the average of $x$ variation
<b>m<sub>l<sup>r</sup></sub></b>	the $r^{\text{th}}$ order light intensity level member set	$\bar{x}_y$	the average of $x$ variation given $y$ set
<b><sup>p</sup>L</b>	the principal light intensity level subset whose member(s) is(are)		

$\varepsilon_x$	the error given the compared $x$ variations		equal to $n_l$
$\sigma_x$	the standard deviation function of $x$ variation	${}^p I^r$	the $r^{\text{th}}$ order principal light intensity level
$\sigma_y$	the standard deviation function of $x$ variation given $y$ set	$P$	the member(s) of the principal light intensity subset
$E(x)$	the expectation of $x$ variation	$r$	the order of the light intensity level
$F(x)$	the cumulative mass function of $x$ variation	$r_0$	the initial order of light intensity level
$\mathfrak{S}_d$	the deviation-based fairness	$s$	the distance of coordinated pairs
$\mathfrak{S}_{net}$	the net fairness		
$\mathfrak{S}_q$	the quadrant-based fairness		
$\alpha$	the ratio of the required pixel(s) to the number of pixel(s)		
$\phi$	the tangent angle of coordinated pairs		
$\eta_r$	the member order density corresponding to the $r^{\text{th}}$ order principal light intensity level		
	$n_{p I^r}$		
$L$	the maximum light intensity level		
$l$	the light intensity level		
$I^r$	the $r^{\text{th}}$ order light intensity level		
$M$	an image width		
$m$	the horizontal coordinate of coordinated pairs		
$N$	an image height		
$n$	the vertical coordinate of coordinated pairs		
$n_l$	the number of pixel(s) corresponding to the light intensity level		
$n_{I^r}$	the number of pixel(s) corresponding to the $r^{\text{th}}$ order light intensity level		
$n_{p I^r}$	the number of pixel(s) corresponding to the $r^{\text{th}}$ order principal light intensity level		
$n_p$	the number of pixel(s)		
$o$	the member order of $\mathbf{m}_1$ from the bottom rank to the top rank, the maximum $o$ at the top rank is		

## 1.2 Background

Actually the image histogram [1], [2], [3] has been used to depict an image histogram components. In different environments the corresponding image histograms from a camera are also different. Any histogram component called the light intensity level  $l$  [1], [2] can depict image details i.e., edges with the lower  $l$ , shades with the maximum  $l$ ,  $L$ . An image histogram can also be utilized to determine whether an image has enough detail to make a good correction<sup>1</sup>. The image histogram can provide a quick picture of the tonal range of any image. Some images have details concentrated in the shadows of weighted lower  $l$ . Some images has details concentrated in the highlights of weighted higher  $l$ . Then an average image has details concentrated in the midtones of weighted medium  $l$ . Generally, an image with full tonal range of  $L$  has some pixels in all areas. To identify the tonal range helps determine appropriate tonal corrections. Besides image details of any histogram component, adaptively clustering pixels geometric features of [4] can capture local image structure. However, [5] emphasized

probability and cumulative density functions categorizing image subclusters.

As described previously, this paper introduces and more precisely demonstrates the principal histogram components of the image histogram to provide important details in an image. With the very low pixels of the principal histogram components, this paper also described the fairness of the pixel distribution to provide the best coverage area of pixels, the experimental results and their analysis with the result parameters for principal image histogram components-based images, and finally conclusions of the characteristics and the benefit of the principal histogram components as the central value of an image.

## 2. Principal Histogram Components

Described in the background the full tonal range of  $L$  can be classified by scenes of shadows, midtones, and highlights. This section presents the principal histogram components explained by the light intensity level  $l$  called the principal light intensity levels.

### 2.1 The principal light intensity levels

Consideration of an image of the resolution of  $M \times N$  equal to all the number of pixel(s) of  $n_p$  pixels the image histogram can depict the number of pixel(s) corresponding to the  $l$ ,  $n_l$ . The  $r^{\text{th}}$  order light intensity level  $l^r$  conformed to the number of pixel(s) corresponding to  $l^r$ ,  $n_{l^r}$ , can be expressed as

$$l^r = \exists(l | l \in \mathbf{L}, \frac{n_{l^r}}{n_p} \geq \frac{n_{l^{r+1}}}{n_p}) \quad (1)$$

where parameters can be denoted below:

- $\mathbf{L}$  the principal light intensity level set whose member(s) is(are)  $l$ s of  $1, 2, 3, \dots, L$ , and
- $r$  the order of light intensity level,  $r = 1, 2, 3, \dots, L$ .

Each of the  $r^{\text{th}}$  order principal light intensity level  ${}^p l^r$ s can be expressed as

$${}^p l^r = \exists(l | l \in \mathbf{L}, \frac{n_{l^r}}{n_p} \geq \frac{n_{l^{r+1}}}{n_p} > \alpha) \quad (2)$$

where parameter can be denoted below:

- $\alpha$  the ratio of the required pixel(s) to the number of pixel(s),  $0 \leq \alpha \leq 1$ .

(2) can be rewritten as

$${}^p l^r = \exists(l^r | l^r \in {}^p \mathbf{L}, \frac{n_{l^r}}{n_p} \geq \frac{n_{l^{r+1}}}{n_p} > \alpha) \quad (3)$$

where parameter can be denoted below:

- ${}^p \mathbf{L}$  the principal light intensity level subset whose member(s) is(are) limited by the maximum light intensity level  $L$ ,  ${}^p \mathbf{L} = \{ {}^p l^1, {}^p l^2, {}^p l^3, \dots, {}^p l^P \}$  the member(s) of the light intensity subset  ${}^p \mathbf{L}$ ,  $P \leq L$ .

### 2.2 Statistics indicators

According to (3), the cumulative mass function of the  $r^{\text{th}}$  order principal light intensity level  $F({}^p l^r)$  of any pixel of the principal light intensity level subset which has the member(s) of  $P$  can be expressed as

$$F(^p l^r) = F(^p l^1 \leq l \leq ^p l^P) = \sum_{r=1}^P n_r > \alpha P \quad (4)$$

where parameter can be denoted below:

$\eta_r$  the member order density corresponding to the  $r^{\text{th}}$  order principal light intensity level,

$$\eta_r = \frac{n_{^p l^r}}{n_p}$$

(1) and (2) infer the following relations  $^p l^r \in l^r$  as well as the principal light intensity level subset limited by  $\mathbf{L}$ ,  $^p \mathbf{L} \subset \mathbf{L}$ . In the definition,  $l$ ,  $l^r$  and  $^p l^r$  of the light intensity level member sets of  $\mathbf{m}_1$ ,  $\mathbf{m}_{l^r}$ , and  $\mathbf{m}_{^p l^r}$  respectively can be placed in similar position in the similar formatted set expressed as

$$\mathbf{m}_1 \triangleq \{l, o, n, m\}, \quad (5)$$

$$\mathbf{m}_{l^r} \triangleq \{l^r, o, n, m\}, \quad (6)$$

and,

$$\mathbf{m}_{^p l^r} \triangleq \{^p l^r, o, n, m\} \quad (7)$$

where parameters can be denoted below:

$o$  the member order of  $\mathbf{m}_1$  from the bottom rank to the top rank, the maximum  $o$  at the top rank is equal to  $n_l$ ,

$n$  the vertical coordinate of coordinated pairs,  $n = 1, 2, 3, \dots, N$ , and

$m$  the horizontal coordinate of coordinate pairs,  $m = 1, 2, 3, \dots, M$ .

(5) informs the first pixel and the last pixel of the black background image of  $l = 1$  as  $\{1, 1, 1, 1\}$  and  $\{1, n_1, N, M\}$ , respectively. In addition, (4) informs the first pixel and

the last pixel of the white background image of  $l = L(256)$  as  $\{L, 1, 1, 1\}$  and  $\{L, n_L, N, M\}$ . Analytically, the average of the member order density  $\eta_r$  in the principal light intensity subset  $^p \mathbf{L}$ ,  $\bar{\eta}_r$ , and the standard deviation<sup>ii</sup> of the member order density  $\eta_r$  in the principal light intensity subset  $^p \mathbf{L}$ ,  $\sigma_{\eta_r}$ , can be expressed as

$$\bar{\eta}_r = \frac{1}{P - r_0 + 1} \sum_{r=r_0}^{P-r_0+1} \frac{n_{^p l^r}}{n_p} > \alpha, \quad (8)$$

and

$$\sigma_{\eta_r} = \sqrt{\frac{1}{P - r_0 + 1} \sum_{r=r_0}^{P-r_0+1} \left( \frac{n_{^p l^r}}{n_p} \right)^2 - (\bar{\eta}_r)^2} \quad (9)$$

where parameter can be denoted below:

$r_0$  the initial order of light intensity level.

(9) shows the dispersion of the member order densities from  $\bar{\eta}_r$  of (7). A low  $\sigma_{\eta_r}$  indicates that any member order density tends to be very close to  $\bar{\eta}_r$  conversely a high  $\sigma_{\eta_r}$  indicates that any member order density  $\eta_r$  is spread out over a large member order density range. In addition, the expectation of the  $r^{\text{th}}$  order principal light intensity level  $^p l^r$  of the principal light intensity subset  $^p \mathbf{L}$ ,  $^p l^r$ , and the standard deviation [6] of the pixel density of the principal light intensity subset  $^p \mathbf{L}$ ,  $\sigma_{^p l^r}$ , can be expressed as

$$E({}^p l^r) = \left( \sum_{r=r_0}^{P-r_0+1} l^r \frac{n_{p_l^r}}{n_p} \right) \left( \sum_{r=r_0}^{P-r_0+1} \frac{n_{p_l^r}}{n_p} \right)^{-1}, \quad (10)$$

$$\sigma_{p_l^r} = \sqrt{\left( \sum_{r=r_0}^{P-r_0+1} ({}^p l^r)^2 \frac{n_{p_l^r}}{n_p} \right) \left( \sum_{r=r_0}^{P-r_0+1} \frac{n_{p_l^r}}{n_p} \right)^{-1} - E^2({}^p l^r)} \quad (11)$$

(11) shows the weighted dispersion of all the  $r^{\text{th}}$  order principal light intensity level(s)  ${}^p l^r$  (s) from  $E({}^p l^r)$  of (10).

### 3. Fairness of Pixel Distribution

Given the member order densities corresponding to the  $r^{\text{th}}$  order principal light intensity level  $\eta_r$ (s) the summation of the number of pixel(s) of that(those) effectively high percentile  $l$ ,  $n_p \sum_{r=1}^P n_r$ , is(are) sufficient to depict the pixel distribution.

#### 3.1 Quadrant-based fairness

To statistically indicate the norm pixel positions, the norm vertical pair  $\bar{n}$  and the norm horizontal pair  $\bar{m}$  of an image are introduced. In addition, the norm of the distance of coordinated pairs  $\bar{s}$  and the norm of the tangent angle of coordinate pairs  $\bar{\phi}$  of all paired pixel positions are introduced. Given the light intensity level member set  $\mathbf{m}_1$  in (4) the  $\bar{s}$  given  $\mathbf{m}_1$ ,  $\bar{s}_{\mathbf{m}_1}$ , and the  $\bar{\phi}$  given  $\mathbf{m}_1$ ,  $\bar{\phi}_{\mathbf{m}_1}$  can be respectively rewritten [6] as

$$\bar{s}_{\mathbf{m}_1} = \sqrt{\left( \sum_{l=1}^L \sum_{o=1}^{n_l} \frac{n-1}{MN} \right)^2 + \left( \sum_{l=1}^L \sum_{o=1}^{n_l} \frac{m-1}{MN} \right)^2}, \quad (12)$$

$$\bar{\phi}_{\mathbf{m}_1} = \arctan \frac{\sum_{l=1}^L \sum_{o=1}^{n_l} n-1}{\sum_{l=1}^L \sum_{o=1}^{n_l} m-1} \quad (13)$$

where parameters can be denoted below:

- $m$  the horizontal coordinate of coordinated pairs of in the given  $\mathbf{m}_1$ , and
- $n$  the vertical coordinate of coordinated pairs of in the given  $\mathbf{m}_1$ .

Conformed to (5), the relation of  $(l, o)$  and  $(m, n)$  in (12) or in (13) is the one-to-one function. And given the  $r^{\text{th}}$  order principal light intensity level member set  $\mathbf{m}_{p_l^r}$  in (7) the  $\bar{s}$  given  $\mathbf{m}_{p_l^r}$ ,  $\bar{s}_{\mathbf{m}_{p_l^r}}$ , and the  $\bar{\phi}$  given  $\mathbf{m}_{p_l^r}$ ,  $\bar{\phi}_{\mathbf{m}_{p_l^r}}$  can be respectively expressed as

$$\bar{s}_{\mathbf{m}_{p_l^r}} = \sqrt{\left( \sum_{r=r_0}^{P-r_0+1} \sum_{o=1}^{n_{p_l^r}} \frac{n-1}{n_p} \right)^2 + \left( \sum_{r=r_0}^{P-r_0+1} \sum_{o=1}^{n_{p_l^r}} \frac{m-1}{n_p} \right)^2}, \quad (14)$$

$$\bar{\phi}_{\mathbf{m}_{p_l^r}} = \arctan \frac{\sum_{r=r_0}^{P-r_0+1} \sum_{o=1}^{n_{p_l^r}} n-1}{\sum_{r=1}^{P-r_0+1} \sum_{o=1}^{n_{p_l^r}} m-1} \quad (15)$$

where parameters can be denoted below:

- $m$  the horizontal coordinate of coordinated pairs of in the given  $\mathbf{m}_{p_l^r}$ , and
- $n$  the vertical coordinate of coordinated pairs of in the

given  $\mathbf{m}_{p1r}$ .

Conformed to (7), the relation of  $(p1r, o)$  and  $(m, n)$  in (14) or in (15) is the one-to-one function. (14) and (12) give the error given the compared distances of coordinated pairs,  $\varepsilon_s$ , equal to  $\bar{s}_{m_{p1r}} - \bar{s}_{m_1}$  and (15) and (13) give the error given the compared tangent angles of coordinated pairs,  $\varepsilon_\phi$ , equal to  $\bar{\phi}_{m_{p1r}} - \bar{\phi}_{m_1}$ . In an image, the quadrant-based fairness  $\mathfrak{F}_q$  with respect to the original coordinated pairs can be expressed [7] as

$$\mathfrak{F}_q = \frac{\bar{s}_{m_{p1r}}}{\varepsilon_s} \frac{\bar{\phi}_{m_{p1r}}}{\varepsilon_\phi} \quad (16)$$

### 3.2 Deviation-based fairness

Given the light intensity level member set  $\mathbf{m}_1$  in (5) the standard deviation of the distance of coordinated pairs  $\sigma_s$  given  $\mathbf{m}_1$ ,  $\sigma_{s_{m_1}}$ , and the standard deviation of the tangent angle of coordinated pairs  $\sigma_\phi$  given  $\mathbf{m}_1$ ,  $\sigma_{\phi_{m_1}}$  can be respectively expressed [7] as

$$\sigma_{s_{m_1}} = \sqrt{\sum_{l=1}^L \sum_{o=1}^{n_l} \frac{(m-1)^2 + (n-1)^2}{MN} - \bar{s}_{m_1}^2}, \quad (17)$$

$$\sigma_{\phi_{m_1}} = \sqrt{\sum_{l=1}^L \sum_{o=1}^{n_l} \frac{\left(\arctan \frac{n-1}{m-1}\right)^2}{MN} - \bar{\phi}_{m_1}^2} \quad (18)$$

And given the  $r^{\text{th}}$  order principal light intensity level member set  $\mathbf{m}_{p1r}$  in (6) the standard deviation of the distance of coordinated pairs  $\sigma_s$  given  $\mathbf{m}_{p1r}$ ,  $\sigma_{s_{m_{p1r}}}$ , and the standard deviation of the tangent angle of coordinated pairs  $\sigma_\phi$  given  $\mathbf{m}_{p1r}$ ,  $\sigma_{\phi_{m_{p1r}}}$  can be respectively expressed as

$$\sigma_{s_{m_{p1r}}} = \sqrt{\sum_{r=r_0}^{p-r_0+1} \sum_{o=1}^{n_{p1r}} \frac{(m-1)^2 + (n-1)^2}{MN} - \bar{s}_{m_{p1r}}^2}, \quad (19)$$

$$\sigma_{\phi_{m_{p1r}}} = \sqrt{\sum_{r=1}^p \sum_{o=1}^{n_{p1r}} \frac{\left(\arctan \frac{n-1}{m-1}\right)^2}{MN} - \bar{\phi}_{m_{p1r}}^2} \quad (20)$$

(19) and (17) give the error given the compared standard deviations of the distances of coordinated pairs,  $\varepsilon_{\sigma_s}$ , equal to  $\sigma_{s_{m_{p1r}}} - \sigma_{s_{m_1}}$  and (20) and (18) give the error given the compared standard deviations of the tangent angles of coordinated pairs,  $\varepsilon_{\sigma_\phi}$ , equal to  $\sigma_{\phi_{m_{p1r}}} - \sigma_{\phi_{m_1}}$ . In an image, the deviation-based fairness<sup>iii</sup>  $\mathfrak{F}_d$  of the  $r^{\text{th}}$  order principal light intensity level member set  $\mathbf{m}_{p1r}$  can be expressed as

$$\mathfrak{F}_d = \frac{\sigma_{s_{m_{p1r}}}}{\varepsilon_{\sigma_s}} \frac{\sigma_{\phi_{m_{p1r}}}}{\varepsilon_{\sigma_\phi}} \quad (21)$$

Thus the net fairness  $\mathfrak{F}_{net}$  of the  $r^{\text{th}}$  order principal light intensity level member set  $\mathbf{m}_{p1r}$  can be expressed as

$$\mathfrak{F}_{net} = \frac{\bar{s}_{\mathbf{m}_{p1r}}}{\varepsilon_s} \frac{\bar{\phi}_{\mathbf{m}_{p1r}}}{\varepsilon_\phi} \frac{\sigma_{s_{\mathbf{m}_{p1r}}}}{\varepsilon_{\sigma_s}} \frac{\sigma_{\phi_{\mathbf{m}_{p1r}}}}{\varepsilon_{\sigma_\phi}} \quad (22)$$

#### 4. Experimental Results and Analysis

The results presented in this section include experimental environment and experimental results subsections. The involved parameters: the light intensity level  $l$ , the  $r^{\text{th}}$  order principal light intensity levels  $^p l^r$ , the quadrant-based fairness  $\mathfrak{F}_q$ , the deviation-based fairness  $\mathfrak{F}_d$ , and the net fairness  $\mathfrak{F}_{net}$  are discussed in both subsections.

##### 4.1 Experimental environment

To evaluate the performance of the experimental results, first the experiments were prepared. From Figure 1 the 128×128 gray scale image of the brain Magnetic Resonance Imaging (MRI) is illustrated. The calculation of the norm of the distance of coordinated pairs  $\bar{s}$ , the norm of the tangent angle of coordinate pairs  $\bar{\phi}$ , the standard deviation of the distance of coordinated pairs  $\sigma_s$  given  $\mathbf{m}_1$ ,  $\sigma_{s_{\mathbf{m}_1}}$ , and the standard deviation of the tangent angle of coordinated pairs  $\sigma_\phi$  given  $\mathbf{m}_1$ ,  $\sigma_{\phi_{\mathbf{m}_1}}$  are illustrated in Table 1. In order to give the accuracy on the performance of static indicators for Figure 1, comparisons of two initial order of light intensity levels of

$r_0 = 1$ ,  $r_0 = 1$  with black holes in the brain, and  $r_0 = 2$  are depicted in Table 1.

Table 1 Initial Parameters for the original gray scale image.

Parameters	Values	Descriptions	Analyzed indicators
$\bar{\phi}_{\mathbf{m}_1}$	45°	$r_0 = 1, P = 256$	$\alpha = 0$
	48.6002°	$r_0 = 1$ (holes), $P = 256$	$\alpha = 0$
	48.6665°	$r_0 = 2,$ $P = 256$	$\alpha = 0$
$\sigma_{\phi_{\mathbf{m}_1}}$	24.0580°	$r_0 = 1, P = 256$	$\alpha = 0$
	11.3244°	$r_0 = 1$ (holes), $P = 256$	$\alpha = 0$
	11.3850°	$r_0 = 2,$ $P = 256$	$\alpha = 0$
$\sigma_{s_{\mathbf{m}_1}}$	52.2542	$r_0 = 1, P = 256$	$\alpha = 0$
	31.2275	$r_0 = 1$ (holes), $P = 256$	$\alpha = 0$
	31.2897	$r_0 = 2,$ $P = 256$	$\alpha = 0$
$\bar{s}_{\mathbf{m}_1}$	89.8026	$r_0 = 1, P = 256$	$\alpha = 0$
	95.6648	$r_0 = 1$ (holes),	$\alpha = 0$

Parameters	Values	Descriptions	Analyzed indicators
		$P = 256$	
	95.8118	$r_0 = 2,$ $P = 256$	$\alpha = 0$
$M$	128	left to right direction	width
$N$	128	top to bottom direction	height
$n_p$	16384	$r_0 = 1, P = 256$ (10464 + 5920)	$\alpha = 0$
$n_p$	5976	$r_0 = 1$ (holes), $P = 256$ (56 + 5920)	$\alpha = 0$
$n_p$	5976	$r_0 = 1$ (holes), $P = 256$	$\alpha = 0$

In the experimental environment, black pixels of  $l=1$  around the brain are discarded. As a result, the reference image of  $r_0 = 1$  with black holes of  $l = 1$  in the brain is similar to Figure 1.  $\bar{s}$  is the hypotenuse line of 95.6648 units in the direction from the top left corner to the bottom right corner and  $\bar{\phi}$  is  $48.6002^\circ$  between  $\bar{s}$  and the adjacent line of  $n = 1$ .  $\sigma_{s_{m_1}}$  of 31.2275 illustrated that coordinated pairs deviated from  $\bar{s}$  and  $\sigma_{\phi_{m_1}}$  of  $11.3244^\circ$  illustrated that any tangent angle of coordinated pairs, deviated from  $\bar{\phi}$ .

**4.2 Experimental results**

The effects of varying the  $r^{\text{th}}$  order principal light intensity levels  $^p l'$ s and the effects of the member(s) of the principal light intensity subset  $P$  can be illustrated in Table 2.

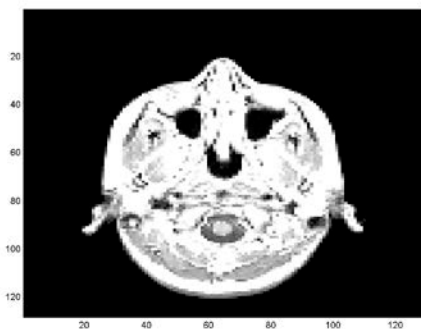


Fig. 1 The original gray scale image of a brain MRI.

Table 2 Result Parameters for Principal Image Histogram Components-Based Images.

Parameters	Values	Descriptions	Analyzed indicators
$\mathfrak{I}_d$	526.9517	$r_0 = 2,$ $P = 2$	$\alpha = 0.1000$
	638.2551	$r_0 = 2,$ $P = 3$	$\alpha = 0.0050$
	91.4615	$r_0 = 3,$	$\alpha = 0.0050$

Parameters	Values	Descriptions	Analyzed indicators
		$P = 3$	
$\mathfrak{S}_{net}$	$3.2684 \times 10^5$	$r_0 = 2,$ $P = 2$	$\alpha = 0.1000$
	$5.4893 \times 10^5$	$r_0 = 2,$ $P = 3$	$\alpha = 0.0050$
	$2.3019 \times 10^5$	$r_0 = 3,$ $P = 3$	$\alpha = 0.0050$
$\mathfrak{S}_q$	620.2439	$r_0 = 2,$ $P = 2$	$\alpha = 0.1000$
	860.0538	$r_0 = 2,$ $P = 3$	$\alpha = 0.0050$
	251.6814	$r_0 = 3,$ $P = 3$	$\alpha = 0.0050$
$\eta_r$	0.1118	$r_0 = 2,$ $P = 2$	$\alpha = 0.1000$
	0.0590	$r_0 = 2,$ $P = 3$	$\alpha = 0.0050$
	0.0062	$r_0 = 3,$ $P = 3$	$\alpha = 0.0050$
$\bar{\phi}_{m_{p1r}}$	$46.3437^\circ$	$r_0 = 2,$ $P = 2$	$\alpha = 0.1000$
	$46.7320^\circ$	$r_0 = 2,$ $P = 3$	$\alpha = 0.0050$
	$53.2535^\circ$	$r_0 = 3,$	$\alpha = 0.0050$

Parameters	Values	Descriptions	Analyzed indicators
		$P = 3$	
$\sigma_{\eta_r}$	0.0000	$r_0 = 2,$ $P = 2$	$\alpha = 0.1000$
	0.0671	$r_0 = 2,$ $P = 3$	$\alpha = 0.0050$
	0.0000	$r_0 = 3,$ $P = 3$	$\alpha = 0.0050$
$\sigma_{\phi_{m_{p1r}}}$	$12.2601^\circ$	$r_0 = 2,$ $P = 2$	$\alpha = 0.1000$
	$12.1665^\circ$	$r_0 = 2,$ $P = 3$	$\alpha = 0.0050$
	$10.4922^\circ$	$r_0 = 3,$ $P = 3$	$\alpha = 0.0050$
$\sigma_{p1r}$	0.0000	$r_0 = 2,$ $P = 2$	$\alpha = 0.1000$
	7.7890	$r_0 = 2,$ $P = 3$	$\alpha = 0.0050$
	0.000	$r_0 = 3,$ $P = 3$	$\alpha = 0.0050$
$\sigma_{s_{m_{p1r}}}$	32.0238	$r_0 = 2,$ $P = 2$	$\alpha = 0.1000$
	31.9507	$r_0 = 2,$ $P = 3$	$\alpha = 0.0050$
	27.4445	$r_0 = 3,$	$\alpha = 0.0050$

Parameters	Values	Descriptions	Analyzed indicators
		$P = 3$	
$\bar{s}_{m p l^r}$	92.5986	$r_0 = 2,$ $P = 2$	$\alpha = 0.1000$
	92.9610	$r_0 = 2,$ $P = 3$	$\alpha = 0.0050$
	100.2220	$r_0 = 3,$ $P = 3$	$\alpha = 0.0050$
$E(p l^r)$	89	$r_0 = 2,$ $P = 2$	$\alpha = 0.1000$
	87.1712	$r_0 = 2,$ $P = 3$	$\alpha = 0.0050$
	54	$r_0 = 3,$ $P = 3$	$\alpha = 0.0050$
$n_p$	1832	$r_0 = 2,$ $P = 2$	$\alpha = 0.1000$
$n_p$	1933	$r_0 = 2,$ $P = 3$	$\alpha = 0.0050$
$n_p$	101	$r_0 = 3,$ $P = 3$	$\alpha = 0.0050$
$p l^1$	1	10464	63.8672%
$p l^2$	89	1832	11.1816%
$p l^3$	54	101	0.6165%
$p l^4$	51	97	0.5920%

Parameters	Values	Descriptions	Analyzed indicators
$p l^5$	64	92	0.5615%

The 2<sup>nd</sup> order principal light intensity level  $p l^2 = 89$  of  $r_0 = 2, P = 2,$  and  $\alpha = 0.1000$  can give high  $\mathfrak{I}_q$  of 620.2439, high  $\mathfrak{I}_d$  of 526.9517, and very high  $\mathfrak{I}_{net}$  of  $3.2684 \times 10^5$  and the result image can be illustrated in Figure 2.

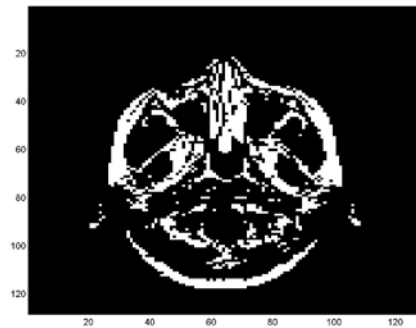


Fig. 2 The  $p l^2 = 89$  image.

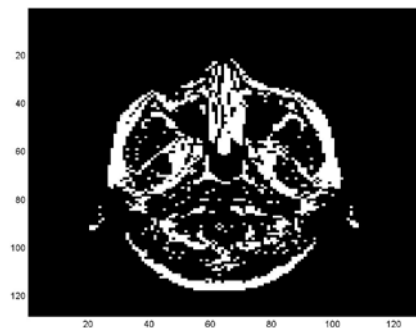


Fig. 3 The  $p l^{2,3} = 89,54$  image.

## 5. Conclusions and Future Works

Any image has its own characteristics. This work provides one of the image characteristics by the utilization of the image giving the main principal light intensity level. The  $r^{\text{th}}$  order principal intensity levels  $^pI^r$  are introduced to describe the scattering of image pixels. The main principal light intensity level obtained from  $^pI^r$  can describe the averaged distance and the averaged tangent angle of image pixels by the quadrant-based fairness. In addition, the main principal light intensity level can also describe the deviation of all distances and the deviation of all tangent angles of all image pixels by the deviation-based fairness. With very low number of pixels of the  $^pI^r$  image the structure of image pixels can be revealed.

In future works, the vertical partitioning-based characteristics of pixels on the image histogram will be researched to reduce the image pixels. Also the sensitivity of the  $r^{\text{th}}$  order principal intensity levels will be considered to select the best central value of an image.

## 6. Acknowledgements

The authors thank the Department of Electrical Engineering and the Department of Computer and Communication Technology, the Faculty of Engineering, Dhurakij Pundit University for their comments and supports, thank the Department of Electrical Engineering, the Faculty of Engineering, Chulalongkorn University for research cooperation and discussion. And, the authors thank the Research Service Center of Dhurakij Pundit University for research supports, and thank the editorial board of the SAU Journal of Science & Technology and the OHEC's reviewers from the Ministry of University Affair for their contributions

and with their valuable suggestions to improve the manuscript.

## References

- [1] B. Homnan and W. Benjapolakul, "Histogram equalization based on cumulative density function, linear function, and pixel position schemes for still image," *Proceeding of IEEE International Conference on System Engineering and Technology*, pp. 1-7, 2012.
- [2] B. Homnan and W. Benjapolakul, "Intermediate Inverse Image Histogram," *Proceeding of IEEE International Conference on Computational Science and Engineering*, pp. 675-679, 2013.
- [3] Adobe. Histograms, <http://help.adobe.com>, 2015.
- [4] K. K. V. Toh and N. A. M. Isa, "Locally Adaptive bilateral clustering for image deblurring and sharpness enhancement," *IEEE Transactions on Consumer Electronics*, vol. 57, no. 3, pp. 1227-1235, 2011.
- [5] B. Homnan and W. Benjapolakul, "Cluster classification characteristics of the critical principal image histogram component," *Proceeding of IEEE International Conference on Electrical Engineering Congress*, pp. 675-679, 2014.
- [6] E. Kreyszig, *Advanced Engineering Mathematics*, John Wiley & Sons, 2011.
- [7] T. H. Cui and P. Mallucci, *Fairness Ideal in Distribution Channels, Dissertation*, University of Minnesota, 2013.

